## Title
A Criterion to Verify Current Distribution Calculations



## Authors
West, A.C.
Sukamto, J.H.
Newman, J.S.

## Publication Date
1989-07-07

UC-210
LBL-27474
Preprint

# Lawrence Berkeley Laboratory
UNIVERSITY OF CALIFORNIA

## Materials & Chemical Sciences Division

Submitted to Journal of the Electrochemical Society

**A Criterion to Verify Current Distribution Calculations**

A.C. West, J.H. Sukamto, and J.S. Newman

July 1989



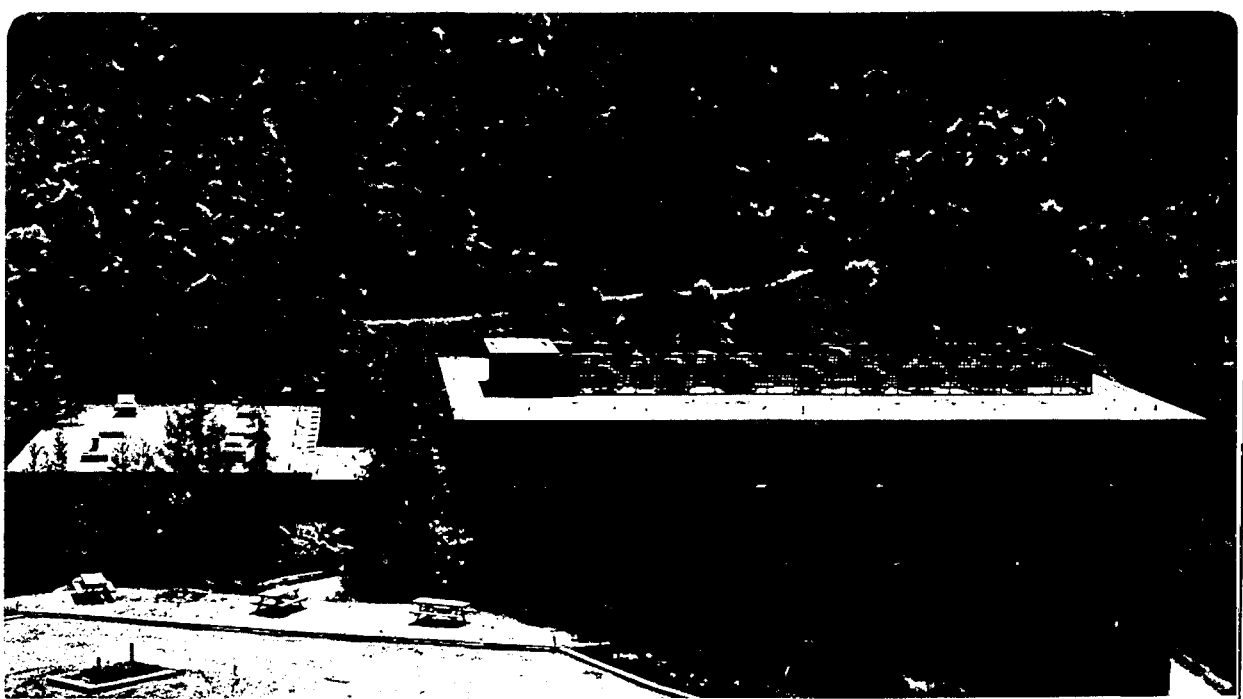

Prepared for the U.S. Department of Energy under Contract Number DE-AC03-76SF00098.

## DISCLAIMER

# A Criterion to Verify Current Distribution Calculations

A.C. West, J.H. Sukamto, and J. S. Newman

Department of Chemical Engineering
University of California

and

Materials and Chemical Sciences Division
Lawrence Berkeley Laboratory
1 Cyclotron Road
Berkeley, CA 94720

July, 1989

LBL-27474

# A Criterion to Verify Current Distribution Calculations

Alan C. West, Johannes H. Sukamto, and John Newman

Materials and Chemical Sciences Division, Lawrence Berkeley Laboratory, and Department of Chemical Engineering, University of California, Berkeley, California 94720

July 7, 1989

## Abstract

Practical uses of the results of the singular-perturbation analysis given by West and Newman are demonstrated. These results are applicable for a large, finite ohmic resistance as compared to the resistance of the interfacial, faradaic reaction. By applying the analysis to a slotted-electrode cell, it is shown how the results can be used to verify the accuracy of numerical results obtained for a specific geometry. The established criterion is valid for the conditions where calculations are most likely to be in error.

## Introduction

This paper provides a practical demonstration of the abstract results of West and Newman [1]. Specifically, it shows how their results provide a criterion by which the validity of current distribution calculations can be tested. Their analysis can be used to determine whether the calculated current density behaves as predicted for a

---

Key words: secondary current distributions, primary current distributions, singular-perturbation analysis

large, finite ohmic resistance (as compared to the resistance of the interfacial reaction). In this paper, the results are applied to a slotted-electrode cell for which the primary current distribution is given by Orazem and Newman [2]. Previously, Smyrl and Newman [3] apply similar results to the rotating disk and flow channel cells.

West and Newman show explicitly how the extreme characteristics of a primary current distribution are approached from a secondary current distribution for an arbitrary angle of intersection between the electrode and insulator. They discuss briefly how this general analysis can be applied to specific cell geometries by checking the validity of other calculations, by extending results, and by aiding in the design of numerical procedures. To generalize the treatment, a parameter $P_o$ is used. It sets the magnitude of the primary current distribution for small distances from the edge:

$$i^p = P_o \, r^{(\pi/2\beta - 1)} \quad . \tag{1}$$

The angle $\beta$ and the radial coordinate $r$ are shown in figure 1. $P_o$ is determined by the cell potential and the details of the entire geometry. It is obtained by comparing the primary current distribution of the cell with equation (1), the asymptotic form valid near the edge.

For large polarization parameters, they show:

1. that the current density deviates from the primary current density where

$$r \approx \left[ \frac{(\alpha_a + \alpha_c) F i_o}{RT\kappa} \right]^{-1} \tag{2}$$

for linear kinetics, and

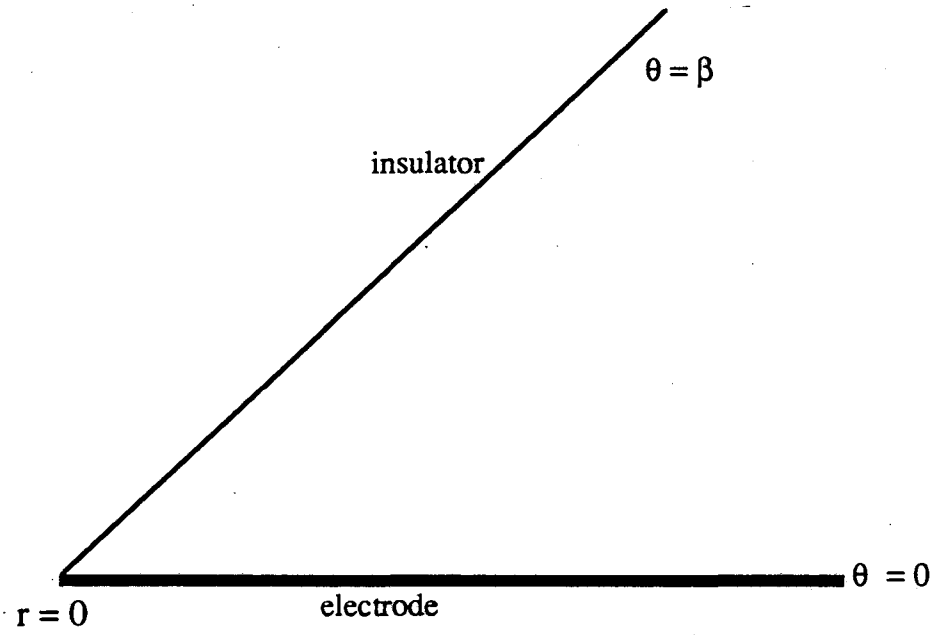


Figure 1. A schematic of the edge region of an electrode and insulator, defining the radial and angular coordinates.

$$r \approx \left[\frac{\alpha_a F P_o}{RT\kappa}\right]^{-2\beta/\pi} \tag{3}$$

for Tafel kinetics.

2. that the current density near an electrode edge behaves as

$$\frac{i_{edge}}{i_{avg}} \propto \left[\frac{(\alpha_a+\alpha_c)Fi_o}{RT\kappa}\right]^{(1 - \pi/2\beta)} \tag{4}$$

for linear kinetics, and

$$\frac{i_{edge}}{i_{avg}} \propto \left[\frac{\alpha_a F P_o}{RT\kappa}\right]^{(2\beta/\pi - 1)} \tag{5}$$

for Tafel kinetics.

3. detailed distributions in the edge region for various angles, $\beta$.

## Numerical Analysis

The primary current distribution of the slotted-electrode cell shown in figure 2 was determined by a technique that utilizes two numerical, Schwarz-Christoffel transformations. Conformal mapping techniques such as this one are often used for the determination of primary current distributions. When coupled with other numerical procedures, problems with more complicated boundary conditions can be analyzed.

Orazem and Newman [2] give the transformation relating the coordinates of figure 2a and figure 2c. Since this is a conformal mapping, Laplace's equation maintains the same form. Insulator boundary conditions also remain the same. Along the counterelectrode, the kinetics are assumed to be infinitely fast, and the constant potential boundary condition is unchanged. At the working electrode, the boundary condition becomes

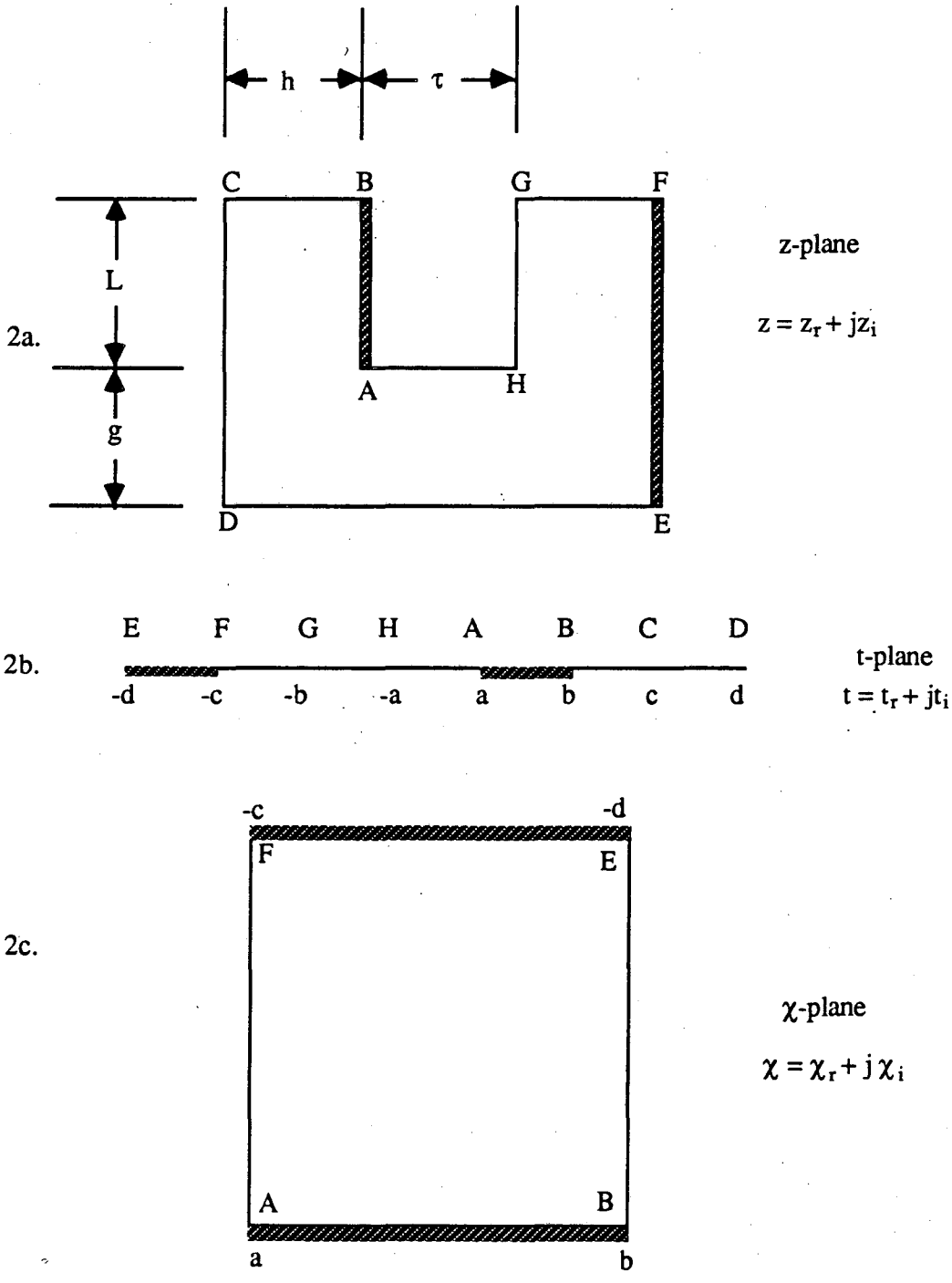


Figure 2. Schematic diagram of the slotted-electrode cell. Figure 2a shows the cell in the original coordinate system. To facilitate solution of Laplace's equation it is mapped conformally to the coordinate system of figure 2c, with the coordinate system shown in figure 2b as an intermediate coordinate system. See reference [2] for details.

$$\frac{\partial \Phi}{\partial \chi_i} = f(\Phi_o)\gamma(\chi), \tag{6}$$

where

$$f(\Phi_o) = -\frac{(\alpha_a+\alpha_c)Fi_o}{RT\kappa}(V - \Phi_o) \tag{7}$$

for linear kinetics, and

$$f(\Phi_o) = -\frac{i_o}{\kappa}\exp\left[\frac{\alpha_a F}{RT}(V - \Phi_o)\right] \tag{8}$$

for anodic, Tafel kinetics.

$\gamma(\chi)$ relates the normal derivatives along the working electrode in the two coordinate systems and is given by

$$\gamma(\chi_r) = \frac{\sqrt{t-a}\,\sqrt{t-a}\,\sqrt{t+a}}{\sqrt{t+b}\,\sqrt{c-t}\,\sqrt{d-t}} \tag{9}$$

where $t$ is related to $\chi$ through

$$\chi = \int_a^t \frac{j\,dt}{\sqrt{t-a}\,\sqrt{t-b}\,\sqrt{t+d}\,\sqrt{t+c}}, \tag{10}$$

and the original coordinate $z$ is related to $t$ through

$$z = \int_0^t \frac{\sqrt{t-a}\,\sqrt{t+a}\,dt}{\sqrt{t-b}\,\sqrt{t+b}\,\sqrt{t-c}\,\sqrt{t+c}\,\sqrt{t-d}\,\sqrt{t+d}}. \tag{11}$$

This problem was solved with a boundary-integral technique. Wagner [4] first suggested such techniques for use in current distribution problems. Our procedure, though, might have more in common with techniques described by Brebbia [5] or by Cahan *et al.* [6]. Newman [7] follows a similar procedure that combines a conformal mapping technique and a boundary-integral method.

In this paper, the geometric ratios used are $L/h = 0.5$, $r/g = 0.1$, and $h/G = 6.0$, where $L$, $h$, $r$, and $g$ are shown in figure 2. The

polarization parameter for linear kinetics is

$$J = \frac{(\alpha_a+\alpha_c)FLi_o}{RT\kappa} \tag{12}$$

and for Tafel kinetics is

$$\delta = \frac{\alpha_a FL|i_{avg}|}{RT\kappa}. \tag{13}$$

The length $L$ used in defining $J$ and $\delta$ is chosen arbitrarily.

## Applicability of the Perturbation Analysis

Singular perturbation analyses can be quite involved. Nevertheless, their results can be simple to use. In this paper, a tool that checks the validity of numerical calculations is established. To use it effectively, one must be aware of the limited range of applicability of the perturbation analysis. Also, a physically significant length should be used in the definitions of the polarization parameters. Otherwise, the coefficients in the series may be very different from unity.

The first neglected term in a perturbation series determines the range of applicability. Because the term arises from the details of the entire cell (and not one specific detail like $\beta$), a general conclusion is difficult to make. To estimate its magnitude, it is useful to study in detail one particular geometry: the disk electrode. For this cell, the characteristic length $L$ in equations (12) and (13) should be replaced with $r_o$, the disk radius.

*Linear Kinetics*—For large $J$, the current density at the electrode edge is given by [8]

$$\frac{i_{edge}}{i_{avg}} = 0.62\ \sqrt{J} + \epsilon^{(2)}\ \frac{\ln J}{\sqrt{J}}, \tag{14}$$

where $\epsilon^{(2)}$ is determined by solving for the second order correction to the primary potential distribution.

The condition for when the first term adequately predicts the current density is

$$\sqrt{J} \gg \frac{\epsilon^{(2)}}{0.62}\ \frac{\ln J}{\sqrt{J}}. \tag{15}$$

Although a determination of $\epsilon^{(2)}$ may not be worth the effort, its value should be near unity, and one can make a reasonable estimate of the range of applicability.

Figure 3 compares calculated values of the current density at the edge of the electrode with the first term of the asymptotic prediction. The predicted behavior is approached by values of $J$ consistent with the above inequality. Equation (14) also suggests an alternate, more sensitive way of plotting results. For example, a plot of $\frac{i_{edge}}{\sqrt{J} i_{avg}}$ *vs.* $\frac{\ln J}{J}$ could be used. For such plots, the ordinate intercept is predicted.

To comment generally about the magnitude of the next term, the relation of Nişancioğlu and Newman [8] is useful:

$$\int_0^1 (1 - \Phi_o/V) r dr = O(\frac{\ln J}{J}) \text{ (for high } J). \tag{16}$$

An analogous term should give the order of the next term for other geometries, and it is expected to be of the same magnitude. If so, for large $J$ and $\beta > \pi/2$,

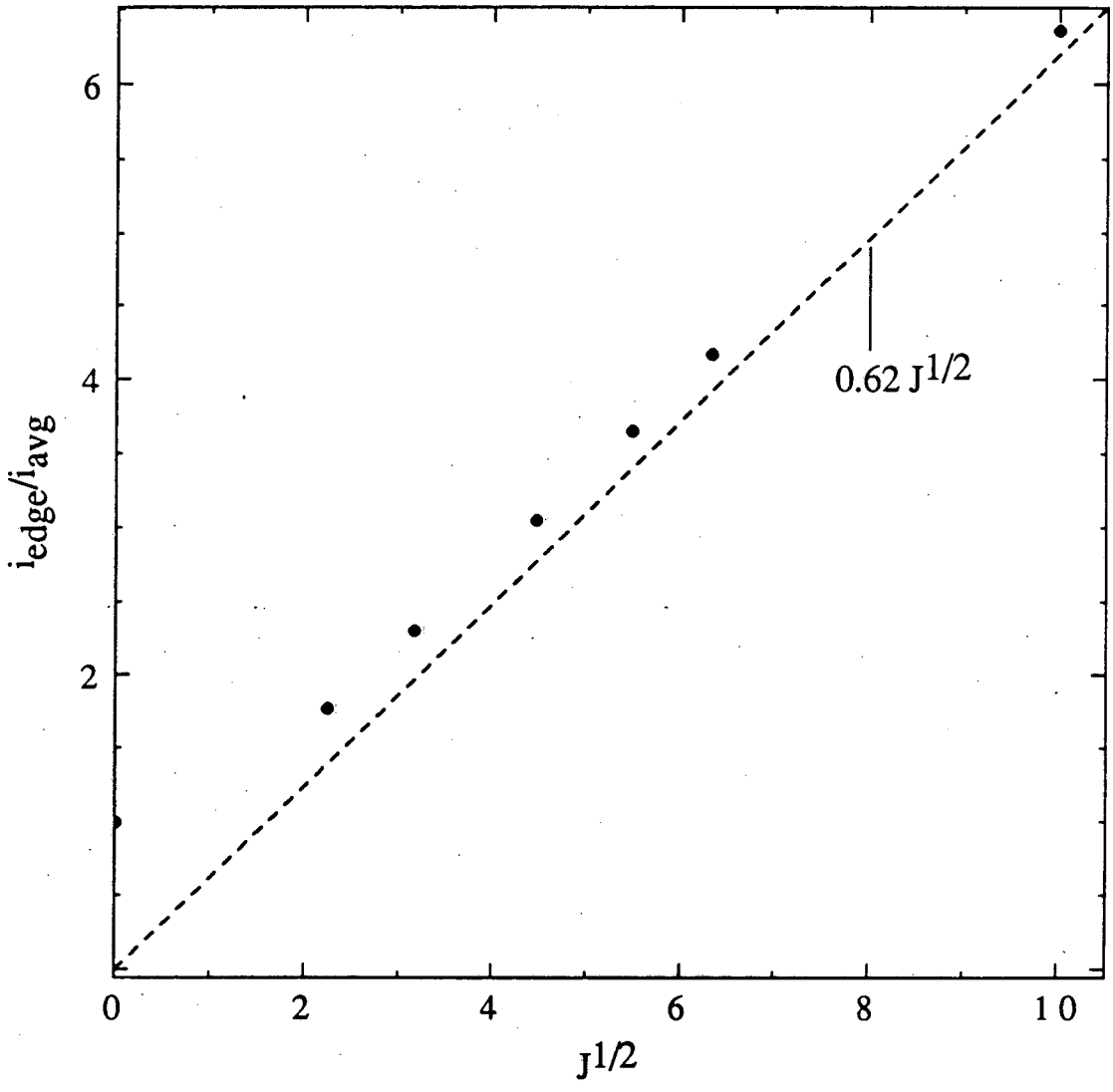


Figure 3. The current density at the edge of a disk electrode for linear kinetics. The points are calculated values, and the dashed line is the asymptotic prediction.

$$\frac{i_{edge}}{i_{avg}} = \epsilon^{(1)} J^{(1-\pi/2\beta)} + \epsilon^{(2)} \frac{\ln J}{J^{\pi/2\beta}} . \tag{17}$$

This implies that the analysis of West and Newman applies when

$$J \gg \frac{\epsilon^{(2)}}{\epsilon^{(1)}} \ln J. \tag{18}$$

*Tafel Kinetics*—For Tafel kinetics on a disk electrode, Appendix A shows that the order of the next term in the perturbation expansion is unity with respect to $\delta$, thus implying that

$$\frac{i_{edge}}{i_{avg}} = 0.196\ \delta + \epsilon^{(2)}. \tag{19}$$

Figure 4 compares the first term with calculated results. In harmony with equation (19), the calculated values lie on a line parallel to the asymptotic prediction. The figure shows that the last data point (near $\delta = 90$) is inaccurate. For larger $\delta$ (not shown), errors are more noticeable. A more sensitive test of numerical calculations would be to plot $\frac{i_{edge}}{\delta i_{avg}}$ *vs.* $1/\delta$, with a predicted ordinate intercept of 0.196.

Appendix A suggests that the next term of a perturbation series will be of order unity for other cell geometries. Previous calculations [9] verify this for the channel geometry (again, $\beta = \pi$). In general, for $\beta > \pi/2$, the expected relationship is

$$\frac{i_{edge}}{i_{avg}} = \epsilon^{(1)}\ \delta^{(2\beta/\pi-1)} + \epsilon^{(2)} . \tag{20}$$

The third term in this series will be of order less than unity. For $\delta^{(2\beta/\pi-1)} > 10$ we can expect the numerical calculations to attain the correct slope but to be offset from a line through the origin by an amount $\epsilon^{(2)}$.

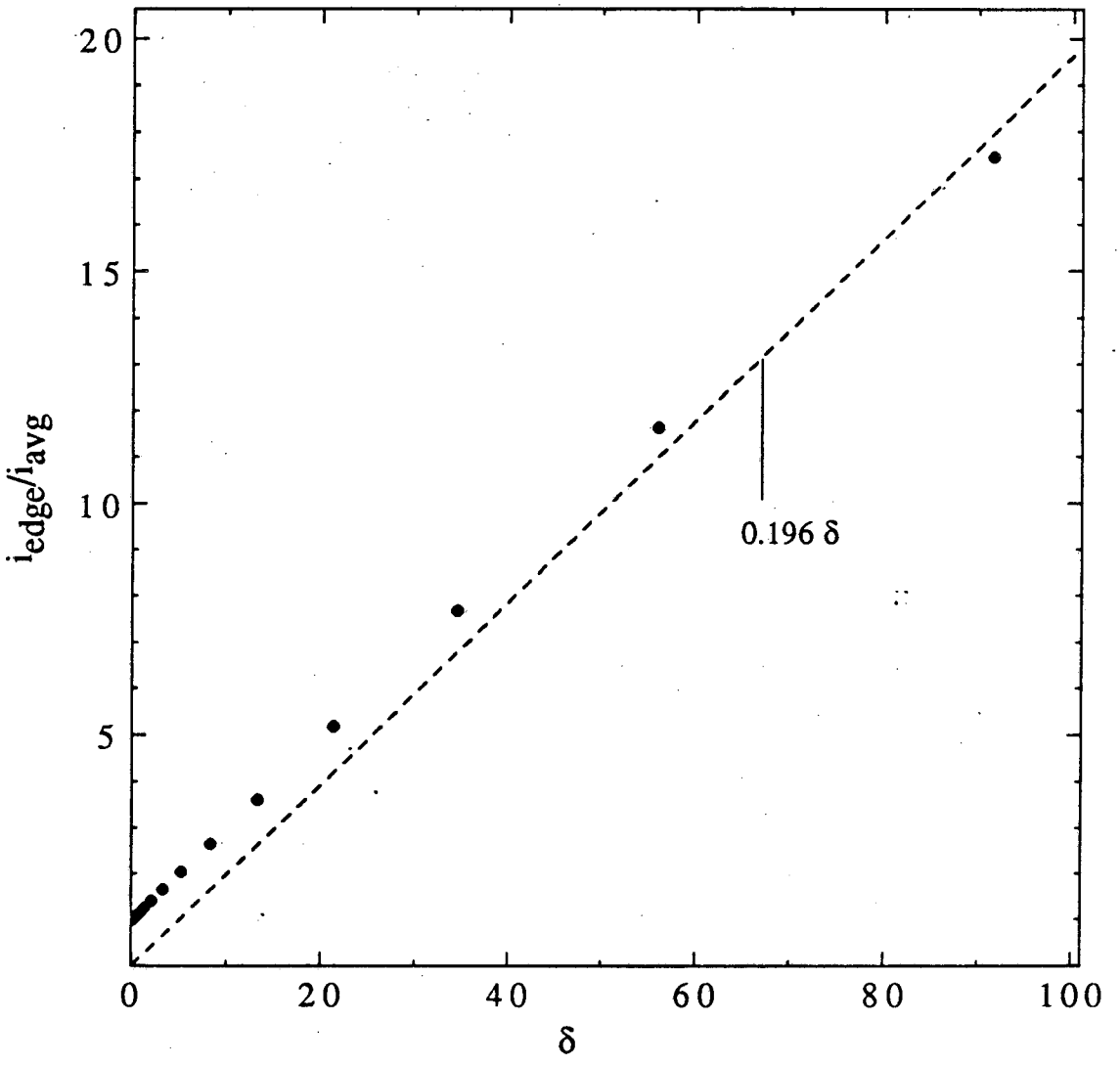


Figure 4. The current density at the edge of a disk electrode for Tafel kinetics. The points are calculated values, and the dashed line is the asymptotic prediction.

## Results and Discussion

For the slotted-electrode cell, the primary current distribution near the electrode edge is

$$i_{as} = P_o r^{-2/3}, \tag{21}$$

where $r$ is the distance along the electrode measured from point $A$. $P_o$ is determined by comparing this asymptotic form with the current distribution as calculated by the method of Orazem and Newman (see figure 5):

$$P_o = 0.569\ L^{2/3} i_{avg}. \tag{22}$$

For linear kinetics in the slotted-electrode cell, equation (28) of West and Newman [1], which is a quantitative statement of the proportionality (3), gives

$$\frac{i_{edge}}{i_{avg}} = 1.5\ J^{2/3} \tag{23}$$

as $J \longrightarrow \infty$. In figure 6 this relationship is compared to calculated values of $i_{edge}/i_{avg}$. Good agreement exists for $J^{2/3} \geq 4$.

For Tafel kinetics, equation (29) of West and Newman gives

$$\frac{i_{edge}}{i_{avg}} = 0.426\ \delta^2 \tag{24}$$

as $\delta \longrightarrow \infty$. Figure 7 compares this relationship with calculated results. An empirical curve, with the predicted slope of 0.426, is fit through the calculated results. Its intercept is determined from the slope of the curve shown in figure 8.

Figure 8 provides a sensitive test of numerical calculations. If the next term in the series is of order unity with respect to $\delta$, the curve should be linear at high $\delta$ and have the ordinate intercept

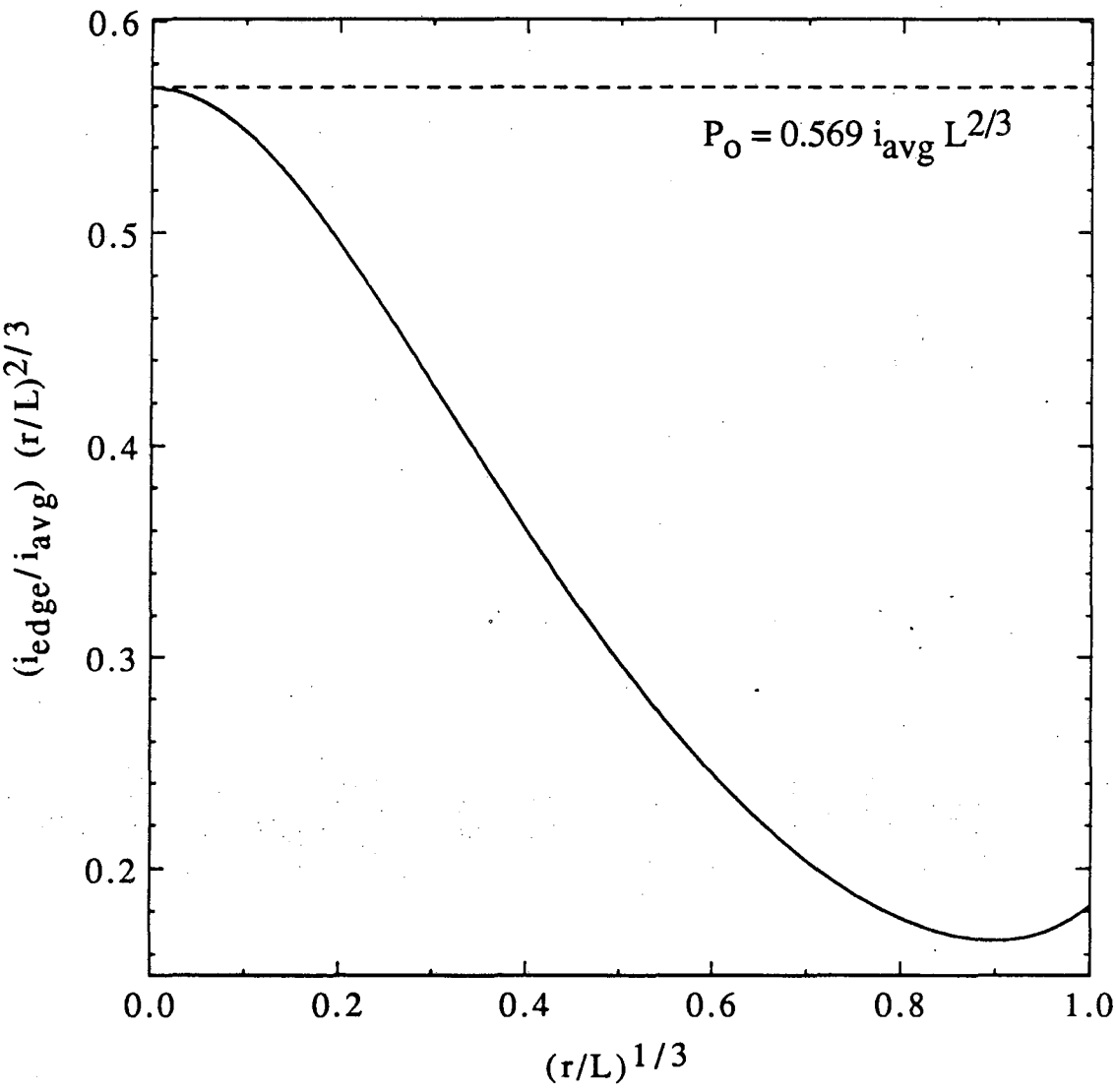


Figure 5. The primary current distribution of a slotted-electrode cell. The dashed line is the asymptotic approximation of the current distribution, given by equation (21).

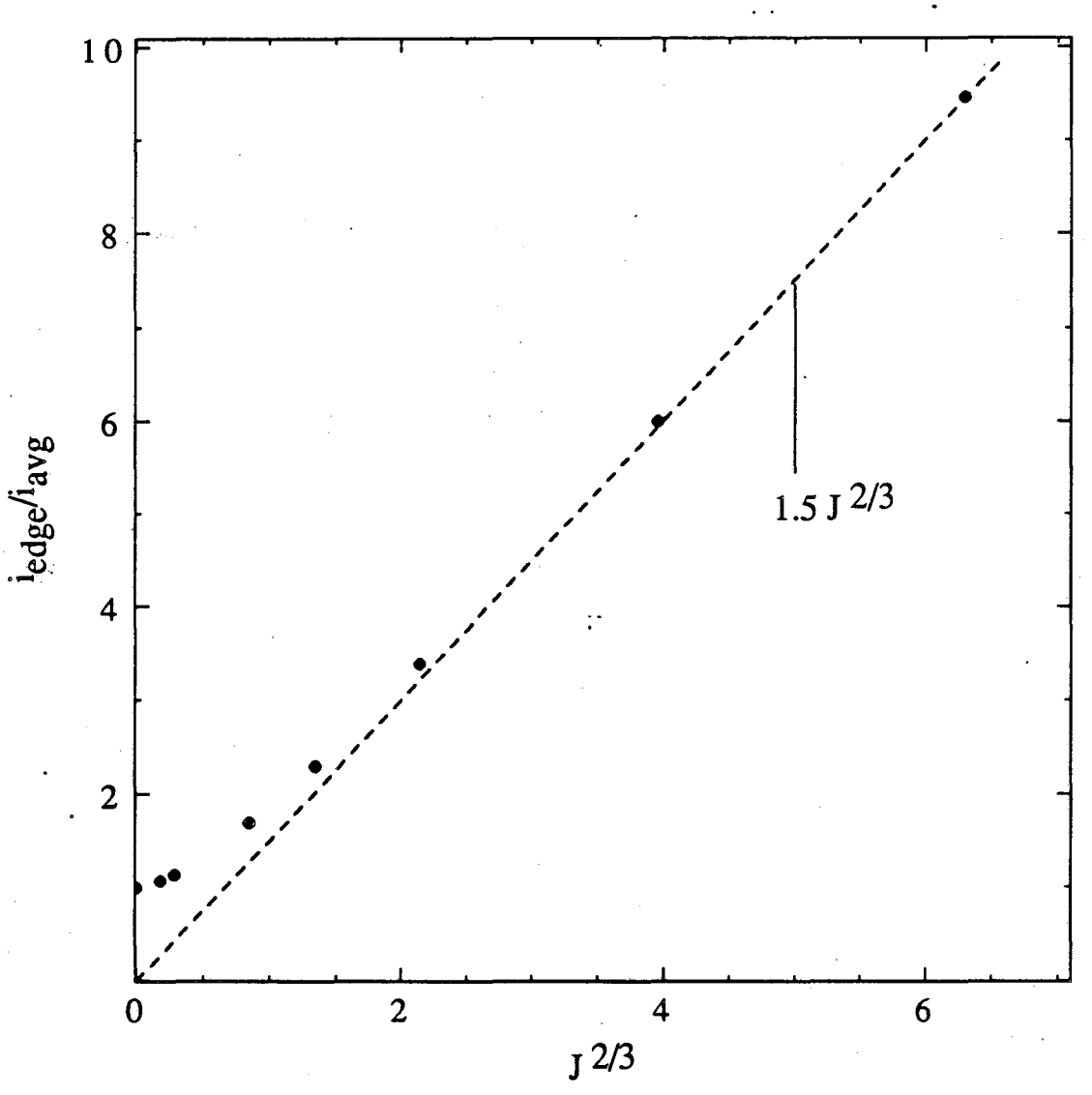


Figure 6. The current density at point *A* of the slotted-electrode cell (figure 2) as it varies with the polarization parameter for linear kinetics. The points are calculated values, and the dashed line is the asymptotic behavior predicted by equation (23).

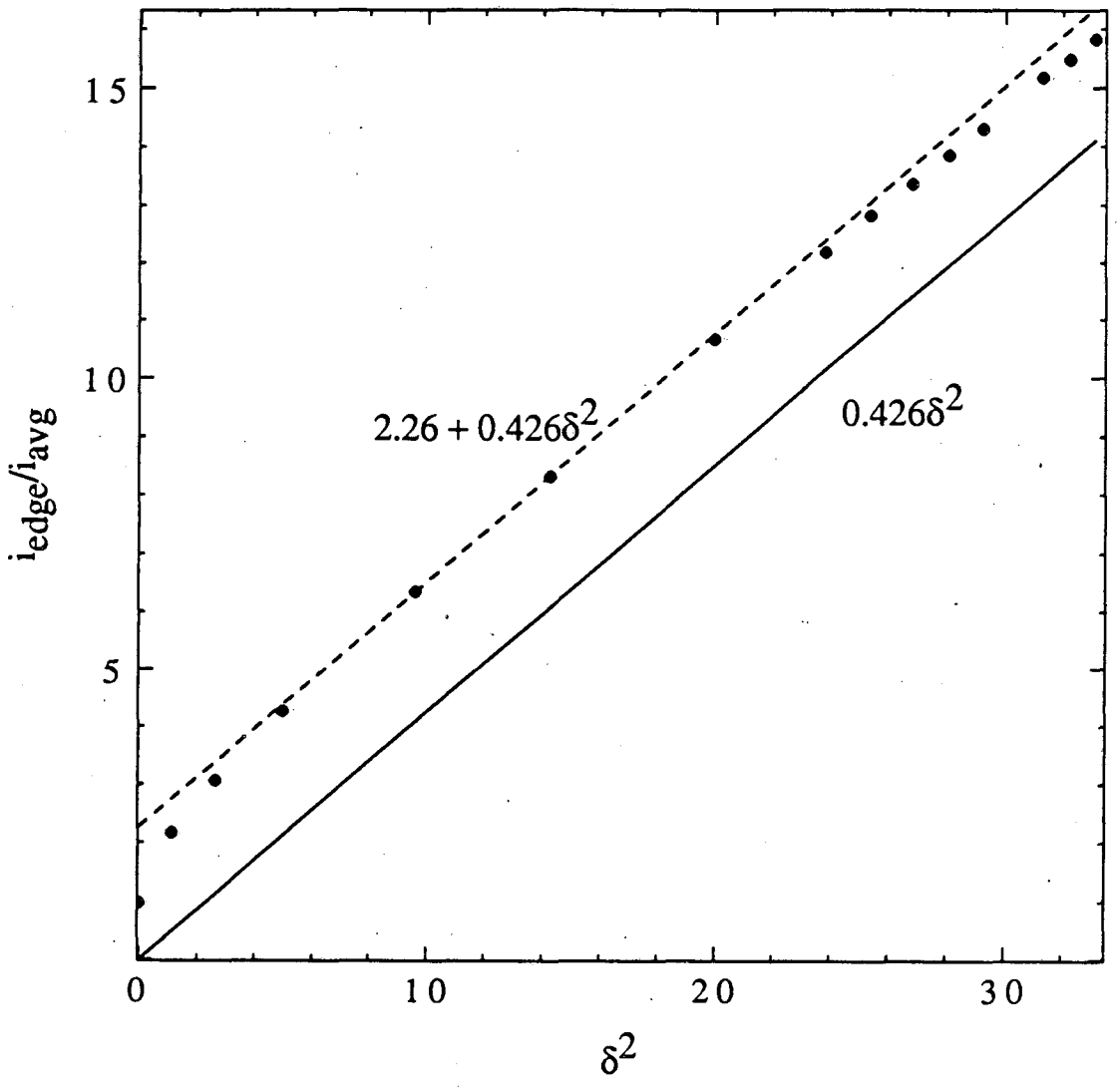


Figure 7. The current density at point *A* of the slotted-electrode cell (see figure 2) as it varies with the polarization parameter for Tafel kinetics. The points are calculated values, the solid line is the asymptotic behavior predicted by equation (24), and the dashed line has the predicted slope but an empirical ordinate intercept.

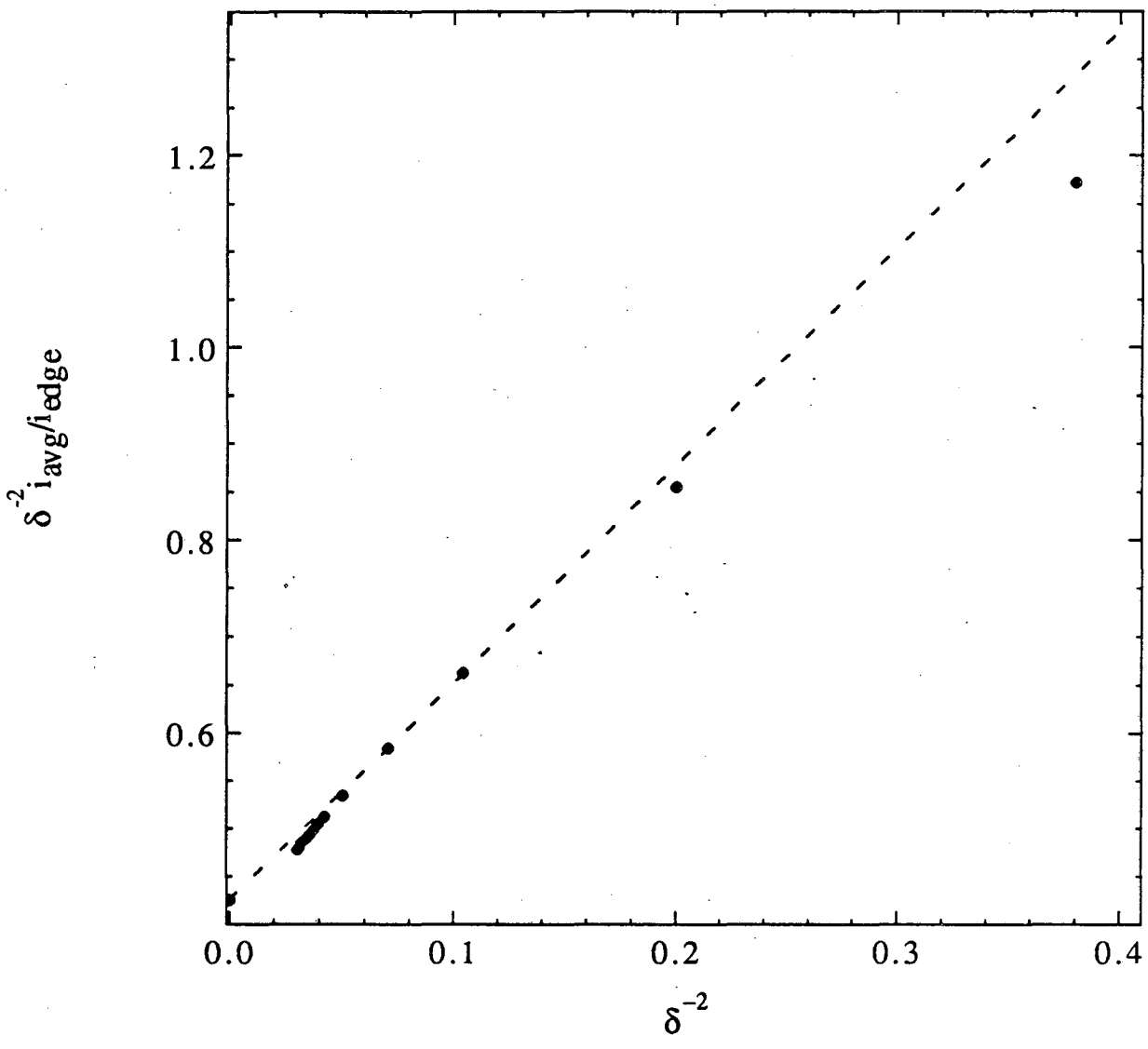


Figure 8. An alternate, more sensitive way of plotting calculated results for Tafel kinetics in the slotted-electrode cell. The ordinate intercept is predicted by the perturbation analysis, and the slope of the line gives an estimate of the next term in the series.

predicted by equation (24). This figure shows that the numerical calculations begin to fail near $\delta^2 = 30$. For larger $\delta$ (not shown), the numerical calculations are clearly in error. The deviation from the semi-empirical curve of figure 7 also suggests that the calculations begin to fail near $\delta^2 = 30$. Our experience suggests that it becomes difficult to obtain highly accurate solutions with traditional numerical procedures when $i_{edge}/i_{avg}$ is much greater than 10.

Figures such as 6, 7, and 8 are recommended as checks on numerical results, where, for large polarization parameters, numerical difficulties arise. To check data quickly, the proportionalities given by equations (3) and (5) can be tested. Deviations from a linear relationship indicate that results are inaccurate.

Few numerical difficulties are expected for small polarization parameters; therefore, a perturbation analysis describing the deviations from a uniform current distribution might not be as interesting. Nevertheless, Appendix B demonstrates by example how the deviations could be predicted. For other geometries, the same functional dependence on the polarization parameter is expected, but general predictions of the coefficients in the series is not possible.

## Conclusions

Applications of the abstract results of West and Newman [1] are demonstrated. Their results, which are valid for asymptotically large polarization parameters, provide a test of numerical results. The predictions do not hold for small polarization parameters, partly because $i_{edge}/i_{avg} = 1$ for a zero polarization parameter. For Tafel kinetics

and obtuse angles of intersection between the electrode and insulator, the next term in a perturbation series is expected to be of order unity. Calculated values of $i_{edge}/i_{avg}$ are expected, therefore, to fall on a line that is parallel to the predictions of West and Newman.

The importance of asymptotic analyses should not be underestimated. In addition to giving insight, they can provide checks on calculations. With the emergence of high-speed computers and sophisticated, packaged software, complicated numerical calculations are more prevalent, and simple tests of these results are necessary.

## Appendix A
## Tafel Kinetics on a Disk Electrode

The order of the next term in a perturbation series describing $i_{edge}/i_{avg}$ for Tafel kinetics on a rotating disk electrode is shown to be unity. It is also suggested that a term of order unity can be expected for other geometries. $O(\epsilon)$ means of order $\epsilon$, and $o(\epsilon)$ means of order lower than $\epsilon$.

Following Smyrl and Newman [3], a potential $\phi$ is defined as

$$\phi = \frac{\pi}{4}\left[1 - \Phi/\Phi_o^p\right] , \tag{A.1}$$

where $\Phi_o^p$ is the primary potential difference, for the same total current, between the disk electrode and a reference electrode placed at infinity. The stretched variables for the outer region (away from the edge of the electrode) are $\tilde{\phi} = \phi$, $\tilde{\eta} = \eta$, and $\tilde{\xi} = \xi$, where $\xi$ and $\eta$ are the rotational elliptic coordinates. In the inner region, the appropriately stretched variables are

$$\bar{\phi} = \delta\phi - \ln\delta, \tag{A.2}$$

$$\bar{\xi} = \delta\xi, \tag{A.3}$$

and

$$\bar{\eta} = \delta\eta. \tag{A.4}$$

The stretched potentials, $\bar{\phi}$ and $\tilde{\phi}$, can be expanded in terms of $\delta$:

$$\tilde{\phi} = \tilde{\phi}^{(0)} + \tilde{f}_1(\delta)\tilde{\phi}^{(1)} + \ldots, \tag{A.5}$$

$$\bar{\phi} = \bar{\phi}^{(1)} + \bar{f}_2(\delta)\bar{\phi}^{(2)} + \ldots. \tag{A.6}$$

Smyrl and Newman show that $\tilde{\phi}^{(0)} = \frac{1}{2}\tan^{-1}\xi$, and they determine numerically $\bar{\phi}^{(1)}$.

In the inner region, terms of order $\delta^{-2}$ are neglected in Laplace's equation. Terms can also arise from the matching and boundary conditions. The insulator boundary condition does not introduce additional terms. Along the disk electrode, the boundary condition is

$$\frac{E}{2}\, e^{\bar{\phi}_o} = \frac{1}{\bar{\eta}}\left(\frac{\partial\bar{\phi}}{\partial\bar{\xi}}\right)_{\bar{\xi}=0}, \tag{A.7}$$

where

$$E = \frac{2i_o}{i_{avg}} \exp\left[\frac{\alpha_a F}{RT}(V - \Phi_o^p)\right]. \tag{A.8}$$

It is shown [3] that

$$\ln E = 1 + \frac{1}{\delta}\ln E^{(1)} + \ldots, \tag{A.9}$$

where $\ln E^{(1)}$ is the second term in a perturbation expansion of $\ln E$.

The boundary condition, therefore, can be rewritten as

$$\frac{e}{2}\left(1 + \frac{1}{\delta}\ln E^{(1)} + o(1/\delta)\right)\exp\left(\bar{\phi}_o^{(1)} + \bar{f}_2(\delta)\bar{\phi}_o^{(2)} + o(\bar{f}_2(\delta))\right) \tag{A.10}$$

$$= \frac{1}{\bar{\eta}}\left\{\left.\frac{\partial\bar{\phi}^{(1)}}{\partial\bar{\xi}}\right|_{\bar{\xi}=0} + \bar{f}_2(\delta)\left.\frac{\partial\bar{\phi}^{(2)}}{\partial\bar{\xi}}\right|_{\bar{\xi}=0} + o(\bar{f}_2(\delta))\right\},$$

which is expanded further to yield

$$\frac{e}{2}\left(1 + \frac{1}{\delta}\ln E^{(1)} + o(1/\delta)\right)\left(1 + \bar{f}_2(\delta)\bar{\phi}_o^{(2)} + \ldots\right)e^{\bar{\phi}_o^{(1)}} \tag{A.11}$$

$$= \frac{1}{\bar{\eta}}\left\{\left.\frac{\partial\bar{\phi}^{(1)}}{\partial\bar{\xi}}\right|_{\bar{\xi}=0} + \bar{f}_2(\delta)\left.\frac{\partial\bar{\phi}^{(2)}}{\partial\bar{\xi}}\right|_{\bar{\xi}=0} + o(\bar{f}_2(\delta))\right\}.$$

Equating terms of the same order in $\delta$ suggests that $\bar{f}_2 = \frac{1}{\delta}$. To decide conclusively necessitates inspecting the matching conditions, where higher order terms due to the outer solution can arise.

In the outer region, the exact form of Laplace's equation (in rotational elliptic coordinates) was solved, and thus no terms arise from the governing equation. Also, no terms arise from the boundary condition at infinity, on the insulator, or on the axis. The boundary condition along the electrode in the outer region can be expressed by

$$\frac{1}{2}Ee^{\delta\bar{\phi}_o} = \frac{1}{\eta}\left.\frac{\partial\bar{\phi}}{\partial\xi}\right|_{\xi=0}. \tag{A.12}$$

Since $\bar{\phi}_o^{(0)} = 0$, this boundary condition is rewritten as

$$\frac{e}{2}\left(1 + \frac{1}{\delta}\ln E^{(1)} + o(1/\delta)\right)\left(1 + \delta\bar{f}_2(\delta)\bar{\phi}_o^{(2)} + \ldots\right)e^{\delta\bar{f}_1(\delta)\bar{\phi}_o^{(1)}} \tag{A.13}$$

$$= \frac{1}{\eta}\left\{\left.\frac{\partial\bar{\phi}^{(0)}}{\partial\xi}\right|_{\xi=0} + \bar{f}_1(\delta)\left.\frac{\partial\bar{\phi}^{(1)}}{\partial\xi}\right|_{\xi=0} + \ldots\right\}.$$

This suggests that $\bar{f}_1 = \frac{1}{\delta}$ and that

$$\bar{\phi}_o^{(1)} = -1 - \ln(\eta), \tag{A.14}$$

which is expected from a straightforward attempt to correct the potential (from the primary potential) for finite electrode kinetics. Smyrl and Newman [3], with a different approach, imply the same results.

$\bar{\phi}^{(1)}$ is described by Laplace's equation in rotational elliptic coordinates:

$$(1 - \eta^2) \frac{\partial^2 \bar{\phi}^{(1)}}{\partial \eta^2} + (1 + \xi^2) \frac{\partial^2 \bar{\phi}^{(1)}}{\partial \xi^2} + 2\xi \frac{\partial \bar{\phi}^{(1)}}{\partial \xi} - 2\eta \frac{\partial \bar{\phi}^{(1)}}{\partial \eta} = 0. \tag{A.15}$$

The insulator boundary condition at $\eta = 0$ is unchanged, the boundary condition at the disk electrode is given by equation (A.14) and $\bar{\phi}^{(1)} \longrightarrow 0$ as $\xi^2+\eta^2 \longrightarrow \infty$. Furthermore, no current should flow to infinity since $\delta$ specifies the total current, and this is supplied by the primary current term, $\bar{\phi}^{(0)}$.

From separation of variables, the solution is

$$\bar{\phi}^{(1)} = \sum_{n=1}^{\infty} B_n P_{2n}(\eta) M_{2n}(\xi), \tag{A.16}$$

where $P_{2n}$ are the even Legendre polynomials, and $M_{2n}$ are Legendre functions of imaginary argument [10]. The $B_n$ are determined through the orthogonality condition:

$$B_n = -(4n + 1) \int_0^1 P_{2n}(\eta) \ln(\eta) d\eta \ . \tag{A.17}$$

The asymptotic behavior (for small $\xi, \eta$) of $\bar{\phi}^{(1)}$ must be developed to provide the matching condition for the inner solution. If $r = (\xi^2+\eta^2)^{1/2}$ and $\theta = \tan^{-1}(\eta/\xi)$, Laplace's equation becomes

$$0 = \left[\frac{\partial^2\bar{\phi}^{(1)}}{\partial r^2} + \frac{1}{r}\frac{\partial\bar{\phi}^{(1)}}{\partial r} + \frac{1}{r^2}\frac{\partial^2\bar{\phi}^{(1)}}{\partial\theta^2}\right]\left[1 + \frac{r^2}{2}(1 - 2\sin^2\theta)\right] \tag{A.18}$$

$$+ \frac{r}{2\sin\theta\cos\theta}\left[\frac{1}{r}\frac{\partial\bar{\phi}^{(1)}}{\partial\theta} - \frac{\partial^2\bar{\phi}^{(1)}}{\partial r\partial\theta}\right]$$

$$+ 2r(1 - 2\sin^2\theta)\frac{\partial\bar{\phi}^{(1)}}{\partial r} - 4\sin\theta\cos\theta\frac{\partial\bar{\phi}^{(1)}}{\partial\theta} .$$

Using a coordinate expansion technique and separation of variables, and applying the appropriate boundary conditions,

$$\bar{\phi}^{(1)} = -1 - \ln r + \bar{A}_1^{(1)} r\cos\theta - r^2\cos^2\theta - \tag{A.19}$$

$$\frac{2}{7}\bar{A}_1^{(1)} r^3\cos\theta + \bar{A}_2^{(1)} r^3\cos(3\theta) + O(r^4),$$

which can be written in terms of $\xi$ and $\eta$ as

$$\bar{\phi}^{(1)}_{(\eta\to 0,\xi\to 0)} = -1 - \ln(\eta^2+\xi^2)^{1/2} + \bar{A}_1^{(1)}\xi - \xi^2 - \tag{A.20}$$

$$\frac{2}{7}\bar{A}_1^{(1)}\xi(\xi^2+\eta^2) + \bar{A}_2^{(1)}\frac{\xi(\xi^2+\eta^2)^{3/2}}{(\xi^2+9\eta^2)^{1/2}} + O((\xi^2+\eta^2)^2).$$

$\bar{A}_1^{(1)}$ and $\bar{A}_2^{(1)}$ would be determined by comparing this asymptotic solution with the complete solution.

Finally, the matching condition is applied. This condition is expressed formally as

$$\frac{\ln\delta}{\delta} + \frac{1}{\delta}\bar{\phi}(\bar{\eta}^2+\bar{\xi}^2\to\infty) = \bar{\phi}(\eta\to 0,\xi\to 0) . \tag{A.21}$$

Agreement must be observed for all orders in $\delta$ and also all orders in $(\xi^2+\eta^2)^{1/2}$. Equation (B-8) of Smyrl and Newman can be rewritten in terms of $\xi$ and $\eta$ as

$$\bar{\phi}(\bar{\eta}^2+\bar{\xi}^2\to\infty) = \frac{\delta}{2}\xi - \ln(E\delta(\eta^2+\xi^2)^{1/2}) + \frac{1}{\delta}\frac{\bar{A}_1^{(1)}\xi}{\xi^2+\eta^2} \tag{A.22}$$

$$+ \frac{1}{\delta}\,\bar{\phi}^{(2)}(\bar{\eta}^2+\bar{\xi}^2\to\infty) + o(1/\delta),$$

where $\bar{A}_1^{(1)}$ is the same as Smyrl and Newman's $A_1$ and is estimated to be -3.1. Substituting for $E$ gives

$$\frac{\ln\delta}{\delta} + \frac{\bar{\phi}(\bar{\eta}^2+\bar{\xi}^2\to\infty)}{\delta} = \frac{\xi}{2} - \frac{1}{\delta}\left[1 + \ln(\eta^2+\xi^2)^{1/2}\right] \tag{A.23}$$

$$+ \frac{1}{\delta^2}\left[\bar{\phi}^{(2)} - \ln E^{(1)} + \frac{\bar{A}_1^{(1)}\xi}{\xi^2+\eta^2}\right] + o(1/\delta^2).$$

To specify completely the matching condition for $\bar{\phi}^{(2)}$, it is necessary to investigate the outer region expansion:

$$\tilde{\phi}(\eta\to 0,\xi\to 0) = \frac{\xi}{2} - \frac{\xi^3}{6} + O(\xi^5) + \frac{1}{\delta}\Big[-1 - \ln(\xi^2+\eta^2)^{1/2} \tag{A.24}$$

$$-\bar{A}_1^{(1)}\xi - \xi^2 + O((\xi^2+\eta^2)^{3/2})\Big] + O(1/\delta^2)$$

The leading term of $\bar{\phi}^{(2)}$ must match the highest unmatched term in $\tilde{\phi}$. Although it might not be worth the effort of solving it, for completeness, the problem statement is given.

The governing equation remains

$$\frac{\partial^2\bar{\phi}^{(2)}}{\partial\bar{\eta}^2} + \frac{\partial^2\bar{\phi}^{(2)}}{\partial\bar{\xi}^2} = 0. \tag{A.25}$$

The insulator boundary condition is

$$\frac{\partial\bar{\phi}^{(2)}}{\partial\bar{\eta}} = 0 \quad \text{at} \quad \bar{\eta} = 0. \tag{A.26}$$

Along the working electrode, the boundary condition is

$$\frac{e}{2}\, e^{\bar{\phi}_o^{(1)}} \left( \ln E^{(1)} + \bar{\phi}_o^{(2)} \right) = \frac{1}{\bar{\eta}} \frac{\partial \bar{\phi}^{(2)}}{\partial \bar{\xi}} \bigg|_{\bar{\xi}=0} , \tag{A.27}$$

where equation (A-18) of Smyrl and Newman gives

$$\ln E^{(1)} = \int_0^\infty \left( \bar{\phi}_o^{(1)} + \ln \bar{\eta} \right) d\bar{\eta} . \tag{A.28}$$

Results of finite-difference calculations can be correlated by

$$\frac{E}{2} = \frac{4.3 + \delta}{4.3 + 0.7358\delta}, \tag{A.29}$$

which is expanded to suggest that $\ln E^{(1)} = -1.544$.

Finally, the matching condition is

$$\bar{\phi}^{(2)}{}_{(\bar{\eta}^2 + \bar{\xi}^2 \to \infty)} = \bar{A}_1^{(1)} \bar{\xi}, \tag{A.30}$$

and, in principle, $\bar{\phi}^{(2)}$ can be obtained.

The next term for $i_{edge}/i_{avg}$ would be

$$\frac{i_{edge}}{i_{avg}} = \frac{e}{2}\, e^{\bar{\phi}_o^{(1)}{}_{(\bar{\eta}=0)}} \left( \delta + \ln E^{(1)} + \bar{\phi}_o^{(2)}{}_{(\bar{\eta}=0)} \right). \tag{A.31}$$

Without further numerical work, the important result is that the next term in a perturbation series is of order unity.

A thorough treatment of the rotating disk geometry is presented. The $E$ parameter of Smyrl and Newman [3] is the key to obtaining the next term in a perturbation series. For other cell geometries, an analogous term arises, and it might be expected to behave similarly. For a coplanar electrode and insulator, a term of order unity seems likely. For other angles of intersection, the correct expansion for the primary current distribution near the edge may cause unforeseen terms to arise. This makes it difficult to draw a more general conclusion.

## Appendix B
## Current Distributions for Small Polarization Parameters

A perturbation analysis describing the deviations from a uniform current distribution is regular. Such an analysis is given here for linear and Tafel kinetics on a disk electrode.

Before proceeding, one should recall the integral equation relating the potential and current distributions on the disk [11]:

$$\Phi_o(r_q) = \frac{2}{\pi\kappa} \int_0^{r_o} \frac{i_n K(m) r}{r + r_q}\, dr \,. \tag{B.1}$$

$K(m)$ is the complete elliptic integral of the first kind [12], and

$$m = \frac{2\sqrt{r r_q}}{r + r_q} \,. \tag{B.2}$$

*Linear Kinetics*—For linear kinetics, the boundary condition along the disk electrode can be expressed as

$$i_n = \frac{(\alpha_a + \alpha_c) F i_o}{RT} (V - \Phi_o) \,. \tag{B.3}$$

We solve this problem as one with a set electrode potential. It is equally valid to specify the total current, as we prefer for Tafel kinetics.

For $J = 0$, the current distribution is uniform, and $\Phi = 0$; that is, the ohmic potential drop in the solution is negligible. This fact, along with equation (B.3), suggests that the potential is appropriately expanded as

$$\frac{\Phi}{V} = J\Phi^{(1)} + J^2\Phi^{(2)} + \ldots \,. \tag{B.4}$$

Substitution of equations (B.3) and (B.4) into equation (B.1) gives a

formal solution for the potential, where terms of the same order in $J$ are equated:

$$\Phi_o^{(1)}(r_q) = \frac{2}{\pi}\int_0^1 \frac{K(m)r}{r + r_q}\,dr\ , \tag{B.5}$$

and, for $n > 1$,

$$\Phi_o^{(n)}(r_q) = -\frac{2}{\pi}\int_0^1 \frac{\Phi_o^{(n-1)}K(m)r}{r + r_q}\,dr\ . \tag{B.6}$$

Nanis and Kesselman [13] show that

$$\Phi_o^{(1)} = \frac{2}{\pi}E(r^2/r_o^2), \tag{B.7}$$

where $E(m)$[†] is the complete elliptic integral of the second kind.

These results give

$$\frac{i_n}{i_{avg}} = 1 + J(\bar{\Phi}_o^{(1)}-\Phi_o^{(1)}) + J^2(\bar{\Phi}_o^{(2)}-\Phi_o^{(1)}\bar{\Phi}_o^{(1)}-\Phi_o^{(2)}) + O(J^3), \tag{B.8}$$

where the $\bar{\Phi}_o^{(n)}$ arise as corrections to the average current density,

$$\bar{\Phi}_o^{(n)} = 2\int_0^1 \Phi_o^{(n)} r dr\ . \tag{B.9}$$

Nanis and Kesselman [13] show that $\bar{\Phi}_o^{(1)} = \frac{8}{3\pi}$.

*Tafel Kinetics*—For Tafel kinetics,

$$i_n = i_o \exp\left[\frac{\alpha_a F}{RT}(V - \Phi_o)\right]. \tag{B.10}$$

For relatively uniform current distributions, Wagner [4] suggests that

---

[†]Note that our argument for the elliptic integral is the square of Nanis and Kesselman's argument. We use a definition of the elliptic integral chosen to be consistent with Abramowitz and Stegun [12].

the Tafel kinetics boundary condition can be linearized:

$$i_n = \frac{\alpha_a F i_{avg}}{RT}\left[\frac{RT}{\alpha_a F} - \Phi_o\right]. \tag{B.11}$$

This suggests that the first correction to a uniform current distribution for Tafel kinetics will be identical to the first correction for linear kinetics (with a properly modified definition of $J$). Only for higher order corrections will differences appear.

We solve this problem by setting $\delta$, the dimensionless average current density. As $\delta \longrightarrow 0$, the current distribution is uniform, and $\Phi$ is zero (as a zeroth approximation). This fact, along with equation (B.10), suggests that the solution potential can be written as

$$\frac{\alpha_a F\Phi}{RT} = \delta\phi^{(1)} + \delta^2\phi^{(2)} + \ldots . \tag{B.12}$$

The electrode potential must also be expanded:

$$\frac{\alpha_a FV}{RT} + \ln\left[\frac{\alpha_a F r_o i_o}{RT\kappa}\right] = \ln\delta + \sum_{n=1} \delta^n V^{(n)}. \tag{B.13}$$

The $\ln\delta$ term on the right side of equation (B.13) can be thought of as the zeroth order term, which is determined by requiring that the dimensionless current distribution be uniform with a magnitude specified by $\delta$. Since this term satisfies the specified average current density, all of the higher order corrections to the potential distribution ($\phi^{(2)}$, *etc.*) must have a zero average current density. This provides the condition to determine $V^{(n)}$.

Following the same procedure used for linear kinetics gives

$$\phi_o^{(1)} = \frac{2}{\pi}\int_0^1 \frac{K(m)r}{r + r_q}\, dr = \frac{2}{\pi} E(r^2/r_o^2), \tag{B.14}$$

$$\phi_o^{(2)} = \frac{2}{\pi} \int_0^1 \frac{K(m)(V^{(1)}-\phi_o^{(1)})r}{r+r_q}\, dr \,, \tag{B.15}$$

and

$$\phi_o^{(3)} = \frac{2}{\pi} \int_0^1 \frac{K(m)\left[V^{(2)}-\phi_o^{(2)}+\frac{1}{2}(V^{(1)}-\phi_o^{(1)})^2\right]r}{r+r_q}\, dr \,, \tag{B.16}$$

where

$$V^{(1)} = 2\int_0^1 \phi_o^{(1)} r dr = \frac{8}{3\pi} \,, \tag{B.17}$$

and

$$V^{(2)} = 2\int_0^1 \phi_o^{(2)} r dr - \int_0^1 (V^{(1)}-\phi_o^{(1)})^2 r dr \,. \tag{B.18}$$

These results give

$$\frac{i_n}{i_{avg}} = 1 + \delta\,(V^{(1)} - \phi_o^{(1)}) + \tag{B.19}$$

$$\delta^2\left[V^{(2)} - \phi_o^{(2)} + \frac{1}{2}(V^{(1)} - \phi_o^{(1)})^2\right] + O(\delta^3).$$

*Summary*—These analyses demonstrate the correct procedure to calculate small deviations from a uniform current distribution. The terms in each series can be obtained by a numerical integration of the previously determined, lower order current distribution. Since $E(1) = 1$, the current density at the edge of the the electrode for linear kinetics is

$$\frac{i_{edge}}{i_{avg}} = 1 + \frac{2}{3\pi} J \quad \text{(small } J\text{)}, \tag{B.20}$$

and for Tafel kinetics is

$$\frac{i_{edge}}{i_{avg}} = 1 + \frac{2}{3\pi} \delta \quad \text{(small } \delta\text{)}. \tag{B.21}$$

As expected [4], the first correction to a uniform distribution is the same for linear and Tafel kinetics. Figure 9 compares numerical results obtained from finite-difference calculations with these asymptotic predictions. The current density at the center of the disk is also compared with its asymptotic value. Since $E(0) = \pi/2$,

$$\frac{i_{center}}{i_{avg}} = 1 + \left( \frac{8}{3\pi} - 1 \right) J \text{ (or } \delta). \qquad \text{(B.22)}$$

These analyses show how the current densities for linear and Tafel kinetics deviate from one another for larger values of the polarization parameter. For other cell geometries, the same linear dependence on $J$ or $\delta$ is expected.

## Acknowledgements

This work was supported by the Assistant Secretary for Conservation and Renewable Energy, Office of Energy Storage and Distribution, Energy Storage Division, U. S. Department of Energy under Contract No. DE-AC03-76SF00098.

## List of Symbols

| | |
|---|---|
| $A_n^{(i)}$ | coefficients arising in matching conditions (see equations (A.19-23)) |
| $a,b,c,d$ | parameters used in the conformal mapping procedures, shown in figure (2), cm |
| $B_n$ | coefficients defined by equation (A.17) |
| $f_n$ | stretching functions for the solution potential |
| $F$ | Faraday's constant, 96487 C/equiv |
| $E$ | parameter defined by equation (A.8) |

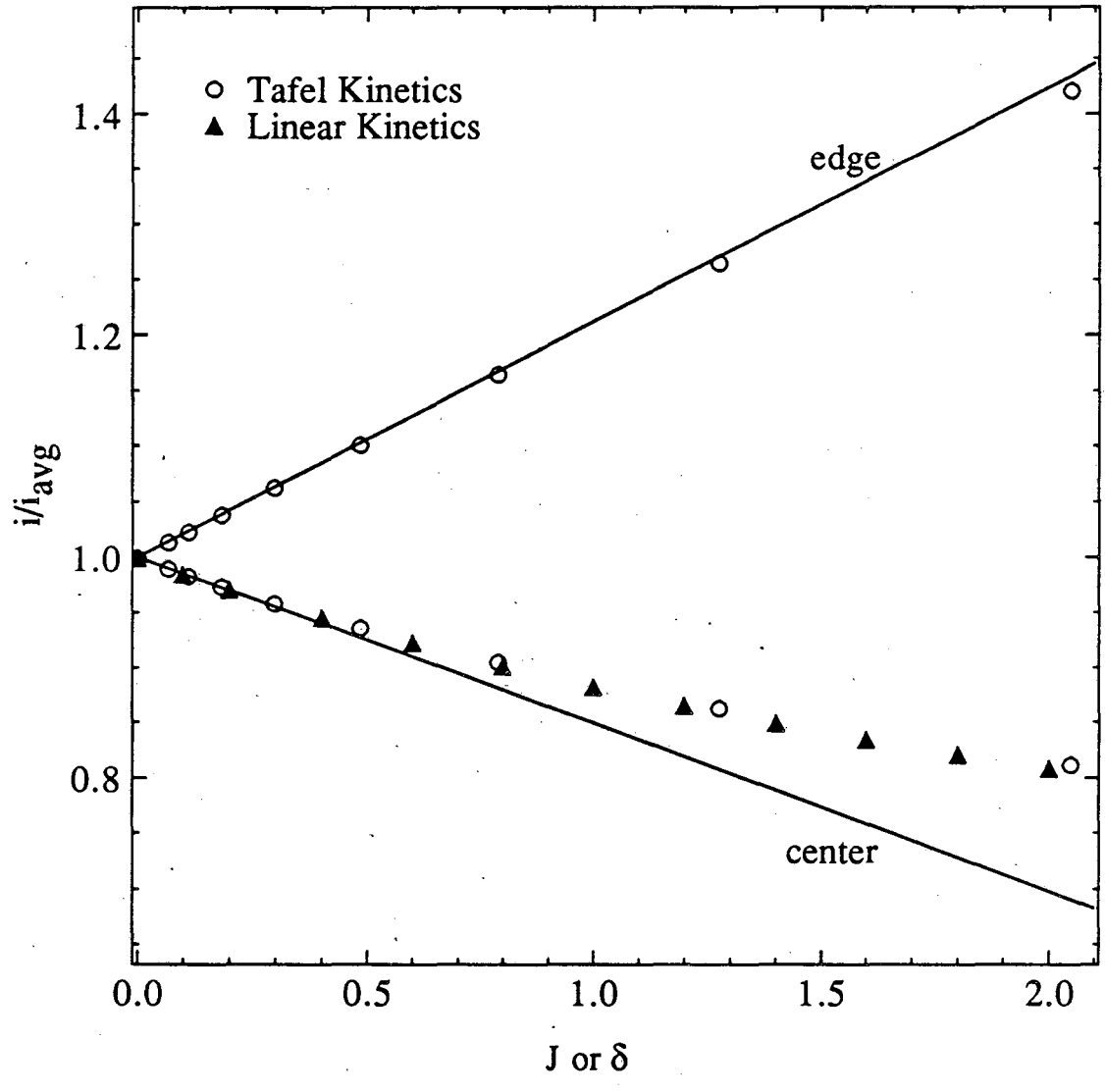


Figure 9. Calculated and predicted current densities for linear and Tafel kinetics at the center and edge of a disk electrode for small polarization parameters. For linear kinetics, the current density depends on $J$, and, for Tafel kinetics, it depends on $\delta$.

| | |
|---|---|
| $E(m)$ | complete elliptic integral of the second kind |
| $i$ | current density, $A/cm^2$ |
| $i_o$ | exchange current density, $A/cm^2$ |
| $j$ | $\sqrt{-1}$ |
| $J$ | dimensionless exchange current density |
| $K(m)$ | complete elliptic integral of the first kind |
| $L,\tau,h,G$ | lengths characterizing the slotted electrode, cm |
| $M_{2n}$ | even Legendre functions of imaginary arguments |
| $P_o$ | parameter defined by equation (1), $A/cm^{(1+\pi/2\beta)}$ |
| $P_{2n}$ | even Legendre polynomials |
| $r$ | radial distance away from the electrode/insulator edge, cm |
| $r_o$ | radius of the disk electrode, cm |
| $r_q$ | radial position at which the potential is being determined, cm |
| $r^*$ | distance where the asymptotic approximation of the primary current distribution is in error by one percent, cm |
| $R$ | universal gas constant, 8.3143 J/mol-K |
| $S$ | stretching variable, $cm^{-1}$ |
| $T$ | absolute temperature, K |
| $t,\chi,z$ | complex coordinates |
| $V$ | electrode potential, V |
| $\alpha_a,\alpha_c$ | transfer coefficients |
| $\beta$ | interior angle between insulator and electrode, radians |
| $\gamma(\chi)$ | relates normal derivatives in original and transformed coordinate systems |
| $\delta$ | dimensionless average current density |
| $\epsilon^{(n)}$ | $n^{th}$ coefficient in a perturbation series |

| | |
|---|---|
| $\eta, \xi$ | rotational elliptic coordinates |
| $\kappa$ | specific conductivity, $\Omega^{-1}cm^{-1}$ |
| $\pi$ | 3.141592654 |
| $\phi$ | dimensionless solution potential |
| $\Phi$ | solution potential, V |
| $\Phi_o$ | solution potential adjacent to the electrode, V |

Subscripts

| | |
|---|---|
| *as* | asymptotic |
| *avg* | average |
| *center* | center of the disk electrode |
| *edge* | electrode/insulator interface |
| *i,r* | imaginary and real parts of a complex variable |

Superscripts

| | |
|---|---|
| p | primary |
| - | inner region variable |
| ~ | outer region variable |

**References**

[1] Alan C. West and John Newman, "Current Distribution Near an Electrode Edge as a Primary Distribution is Approached," *J. Electrochem. Soc.*, in press, (1989).

[2] Mark E. Orazem and John Newman, "Primary Current Distribution and Resistance of a Slotted-Electrode Cell," *J. Electrochem. Soc.*, 131, 2857 (1984).

[3] William H. Smyrl and John Newman, "Current Distribution at Electrode Edges at High Current Densities," *J. Electrochem. Soc.*, 136, 132 (1989).

[4] Carl Wagner, "Theoretical Analysis of the Current Density Distribution in Electrolytic Cells," *J. Electrochem. Soc.*, 98, 116 (1951).

[5] C. A. Brebbia, *The Boundary Element Method for Engineers*, John Wiley and Sons, New York (1978).

[6] B. D. Cahan, Daniel Scherson, and Margaret A. Reid, "I-BIEM. An Iterative Boundary Integral Equation Method for Computer Solutions of Current Distribution Problems with Complex Boundary Conditions—A New Algorithm," *J. Electrochem Soc.*, 135, 285 (1988).

[7] John Newman, "Engineering Design of Electrochemical Systems," *Ind. Eng. Chem.*, 60, no. 4, 12 (1968).

[8] Kemal Nişancioğlu and John Newman, "The Short-Time Response of a Disk Electrode," *J. Electrochem. Soc.*, 121, 523 (1974).

[9] William R. Parrish and John Newman, "Current Distribution on Plane, Parallel Electrodes in Channel Flow," *J. Electrochem. Soc.*, 117, 43 (1970).

[10] John Newman, "Current Distribution on the Rotating Disk below the Limiting Current," *J. Electrochem. Soc.*, 113, 1235 (1966).

[11] John Newman, "The Fundamental Principles of Current Distribution and Mass Transport in Electrochemical Systems," in *Electroanalytical Chemistry*, A. J. Bard, Editor, pp. 187-351, Marcel Dekker, Inc., New

York (1973).

[12] M. Abramowitz and I. A. Stegun, eds., *Handbook of Mathematical Functions*, National Bureau of Standards, Washington (1964).

[13] Leonard Nanis and Wallace Kesselman, "Engineering Applications of Current and Potential Distributions in Disk Electrode Systems," *J. Electrochem. Soc.*, 118, 454 (1971).

LAWRENCE BERKELEY LABORATORY
TECHNICAL INFORMATION DEPARTMENT
1 CYCLOTRON ROAD
BERKELEY, CALIFORNIA 94720